



Highly efficient removal of Pb(II) ion from aqueous phase using surface-modified graphene: equilibrium and kinetic study

Mukarram Zubair^a, Nabeel Jarrah^{a,b,*}, Mohammad Saood Manzar^a,
Mamdouh A. Al-Harthy^{c,d}, Nuhu Dalhat Mu'azu^a

^aDepartment of Environmental Engineering, University of Dammam, Dammam 31451, Saudi Arabia, Tel. +966596087655; email: najarrah@uod.edu.sa (N. Jarrah), Tel. +966562149458; email: mzzubair@uod.edu.sa (M. Zubair), Tel. +966556860314; email: msmanzar@uod.edu.sa (M.S. Manzar), Tel. +966507532689; email: nmdalhat@uod.edu.sa (N.D. Mu'azu)

^bDepartment of Chemical Engineering, Mutah University, Karak 61710, Jordan

^cDepartment of Chemical Engineering, King Fahd University of Petroleum and Minerals, Dhahran 31261, Saudi Arabia, Tel. +966565337770; email: mamdouh@uod.edu.sa

^dCenter of Research Excellences in Nanotechnology, King Fahd University of Petroleum and Minerals, Dhahran 31261, Saudi Arabia

Received 8 November 2016; Accepted 19 April 2017

ABSTRACT

A novel surface-modified graphene (SMG) was employed as an adsorbent for the removal of Pb(II) from aqueous solution at room temperature (295 ± 5 K). The SMG was prepared from graphene (G) via oxidation method using concentrated nitric acid. Scanning electron microscopy, thermogravimetric analysis, Brunauer, Emmett, and Teller, and Fourier transform infrared spectroscopy were used to characterize the produced adsorbent. Batch adsorption experiments were carried out under different operating conditions; pH (2–7), adsorbent dosage (4–32 mg), and contact time (5–240 min). The maximum Pb(II) adsorption was obtained at a pH of 6, adsorbent dose of 20 mg after 100 min at 298 K. Surface of the SMG had more oxygen functionalities and higher surface area compared with the G, thereby resulting in enhanced removal of Pb(II), significantly. Pseudo-second-order kinetic model fitted the results better than pseudo-first-order and intra-particle diffusion models. Redlich–Peterson, Freundlich, and Langmuir isotherm models fitted very well the equilibrium results. The SMG was a superior adsorbent for Pb(II) with a maximum adsorption capacity of 140 mg/g. Therefore, it can be concluded that SMG can be effectively used to remove heavy metals from waste and domestic water.

Keywords: Adsorption; Lead; Modified graphene; Isotherm and kinetic models

1. Introduction

Presence of toxic metals in wastewater and domestic water beyond the consent limit has been an issue of great concern due to the potential harming effect on human health and environment [1,2]. Lead is listed among priority pollutants [3,4] and its tolerable limit in drinking water allowed by US Environmental Pollution Agency is 0.015 mg/L [5]. Lead ions

are released into the environment from various industries such as mining, tanneries, metal plating, and other industrial emissions [2]. Various techniques such as precipitation [6], flocculation [7], ion exchange [8], membrane separation [9], and adsorption [10] are utilized to get rid of toxic heavy metals. In comparison to other treatment methods, adsorption is found to be more effective and cheap in remediation of trace metals. Nevertheless, selection of appropriate adsorbent and operating conditions has been the key step to achieve maximum efficiency in adsorption process. Activated carbon [11], zeolite [12], and bentonite [13] have been reported for the

* Corresponding author.

removal of Pb(II) from aqueous solutions. Yet, due to their low adsorption efficiency, researchers are still doing efforts to develop superior adsorbents that exhibit higher uptake capacity and capture broad range of pollutants with good chemical and thermal stability.

Graphene, a unique two-dimensional densely packed honeycomb crystal lattice, possesses remarkable properties such as high surface area, excellent chemical stability, and good thermal and mechanical properties attracted demanding interest in different applications such as polymer nanocomposites [14–17], transparent electrodes [18], and organic photovoltaic devices [19].

Graphene and its derivatives exhibited outstanding adsorbent characteristics due to its high surface area and presence of functional groups on its surface and provides a new window of research for effective wastewater treatment [20–24]. Recently, graphene and its derivatives have been utilized for the removal of Pb(II) and Cd(II) [25], Cr(VI) [26], and anionic and cationic dyes [24]. Surface modification of carbonaceous materials such as activated carbon, carbon nanotubes (CNT), carbon nanofibers, and graphene using different chemicals and techniques provide various additional surface functional groups like carboxylic, carboxyl, hydroxyl, and metal oxides on their surfaces [27].

These functional groups act as active adsorption sites thereby improving the interaction and effective bonding with pollutants; consequently, enhancing the uptake capacity for various pollutants [25,26,28,29]. Performances of heavy metals sorption on carbonaceous material systems have been demonstrated to be significantly improved via appropriate surface modification of the sorbent materials [30–32].

Recently, Ihsanullah et al. [33] modified activated carbon, CNT, and carbon fiber using nitric acid and found significant improvement in adsorption capacity for Cr(VI) ion. Wang et al. [34] also reported enhanced adsorption capacity of Pb(II) on tartaric acid-modified graphene. However, to the best of our knowledge based on extensive literature review, no study was found to have investigated the utilization of acid-modified graphene for adsorption of Pb(II) ions from aqueous solution. Therefore, the main objective of this study was to investigate the adsorption performance of Pb(II) on surface-modified graphene (SMG) prepared via chemical oxidation using nitric acid. The morphology, surface area, and surface functional groups of adsorbents were examined using scanning electron microscopy (SEM); Brunauer, Emmett, and Teller (BET), thermogravimetric analysis (TGA), and Fourier transform infrared spectroscopy (FTIR),

respectively. Adsorption batch study was undertaken to investigate the effect of influential parameters such as pH, adsorbent dose, and contact time. The experimental results were fitted using equilibrium isotherms (i.e., Langmuir model, Freundlich, and Redlich–Peterson model) and kinetic models (i.e., pseudo-first-order, pseudo-second-order, and intra-particle diffusion).

2. Experimental section

2.1. Materials and reagents

Graphene (G) with size of 50 nm was purchased from the Grafen Chemical Industries Co. (Turkey). The lead ion stock solution was prepared using pure Pb(NO₃)₂ in ultrapure water. All chemicals (NaOH, HCl, and HNO₃) were analytical grade purchased from Sigma Aldrich (USA).

2.2. Surface modification

Surface modification of graphene was performed via thermal oxidation method [35]. About 1 g of graphene was boiled in 150 mL of HNO₃ (69%, AnalaR grade) at 120°C for about 48 h with continuous reflux to accomplish maximum oxidation. After reaction, the mixture was cooled and diluted with ultrapure water and vacuum-filtered through 1 μm cellulose acetate filter paper. The mixture was repeatedly washed with deionized water until the pH of 7 was reached. Finally, the SMG was dried at 40°C for 24 h.

2.3. Characterization

The surface characteristics of raw and SMG were published in our previous study [35]. For clarity reasons, Table 1 summarizes some of these surface properties of graphene (G) and SMG. The surface morphology of adsorbents was examined by SEM using Tescan mira-3 FE-SEM. TGA was performed on Q-600 TA instrument at heating rate of 10°C/min. BET surface area and pore size were obtained using ASAP 2020 Micromeritics. FTIR of SMG was analyzed before and after Pb(II) adsorption using Nicolet 6700 spectrometer with resolution of 4 cm⁻¹.

2.4. Pb(II) batch adsorption studies

Batch adsorption study was performed to investigate the effect of different parameters on the adsorption of Pb(II) by raw and modified graphene. In this study, the

Table 1
Surface properties of graphene (G) and surface-modified graphene (SMG) [35]

Technique	G	SMG
FTIR	Presence of peak at 3,445 and 1,638 cm ⁻¹ corresponds to hydroxyl group and C=C group of graphene, respectively	New peaks at 1,260, 1,102, and 1,016 cm ⁻¹ correspond to C–O–C, C–OH, and C–O groups, respectively
XRD	Diffraction peak detected at 26.9° Layer to layer spacing estimated through Bragg's equation is 0.33 nm	Diffraction peak shifted to at 21.6° after oxidation Layer to layer spacing is 0.47 nm
XPS	Sp ³ (19%), C=O (2.4%), O–C=O (1.2%), π–π (7%)	Sp ³ (19.4%), C=O (3%), O–C=O (1.7%), π–π (7.3%)

effect of pH (2–7), adsorbent dosage (4–32 mg), and contact time (5–240 min) was investigated. The experiments were performed by mixing 10 mg of raw or modified graphene (except in case of adsorbent dose effect) with 40 mL of 20 mg/L of Pb(II) solution in 50 mL round bottom plastic tubes at 250 rpm. The tubes were shaken for 180 min (except in the kinetic study) to reach equilibrium and then filtered using 40 μm cellulose acetate filters. The pH of solutions was adjusted using 0.1 N HNO_3 and 0.1 N NaOH. Atomic absorption spectrophotometer (Thermo Scientific iCE 3000 Series) was used to measure the concentration of Pb(II) before and after treatment.

The equilibrium adsorption capacity q_e (mg/g) and the percentage removal were calculated using the following equations:

$$\text{Adsorption capacity } (q_e) = \frac{C_o - C_e}{W} \times V \quad (1)$$

$$\text{Percentage removal} = \frac{C_o - C_e}{C_o} \times 100 \quad (2)$$

where C_o and C_e are the initial and equilibrium concentration (mg/L) of Pb(II) ion, q_e (mg/g) is the equilibrium adsorption capacity, W (g) is the weight of the adsorbent, and V (L) is the volume of solution.

2.5. Kinetic modelling

The two common models used to study the mechanism of the surface reaction are pseudo-first-order (Eq. (3)) and pseudo-second-order (Eq. (4)) models [36]. Pseudo-first-order fits the data when physisorption takes place, while pseudo-second-order explains the data if chemisorption is controlling the surface reaction. Moreover, intra-particle diffusion model (Eq. (5)) was employed to investigate the role of the internal diffusion during the process.

$$\text{Pseudo-first-order model: } \ln(q_e - q_t) = \ln q_e - k_1 t \quad (3)$$

$$\text{Pseudo-second-order model: } \frac{t}{q_t} = \frac{t}{k_2 q_e^2} + \frac{t}{q_e} \quad (4)$$

$$\text{Intra-particle diffusion: } q_t = k_3 t^{0.5} + C \quad (5)$$

where q_e and q_t are the adsorption capacity of Pb(II) on G and SMG at equilibrium and time (t), respectively. The other parameters are the constants of the models. One can calculate these parameters by plotting Eqs. (3)–(5) as presented in Fig. 8. The parameters and correlation coefficients (R^2) of the three models are calculated using linear square method and are listed in Table 3.

2.6. Equilibrium modelling

In order to understand comprehensively how the Pb(II) ions are adsorbed on surface of G and SMG and the nature of interaction between adsorbate and adsorbents, equilibrium data were employed on the most commonly used isotherm models namely Freundlich, Langmuir, and Redlich–Peterson isotherms:

$$\text{Langmuir isotherm model: } \frac{C_e}{q_e} = \frac{1}{b} q_m + \frac{C_e}{q_m} \quad (6)$$

$$\text{Freundlich isotherm model: } \ln q_e = \ln K_f + \frac{1}{n} \ln C_e \quad (7)$$

Redlich–Peterson isotherm model:

$$\ln(K_R \frac{C_e}{q_e} - 1) = b_R \ln C_e + \ln a_R \quad (8)$$

where C_e (mg/L) is the equilibrium concentration of adsorbent, q_e (mg/g) is the amount of Pb(II) adsorbed at equilibrium. The other parameters are constants of the models, which can be calculated by fitting the experimental data using linear form of the isotherms (Eqs. (6)–(8)). For Langmuir isotherm, q_m (mg/g) is the maximum adsorption capacity and b is the Langmuir constant [37]. Dimensionless factor R_L is an equilibrium parameter that can be calculated using Eq. (9). Adsorption is favourable, but reversible when $0 < R_L < 1$, and unfavourable at $R_L = 0$, 1, and >1 [38].

$$R_L = \frac{1}{1 + bC_o} \quad (9)$$

3. Results and discussion

3.1. Structural characterization of graphene

Table 1 illustrates the summary of surface characteristic (XRD, X-ray photoelectron spectroscopy (XPS), and FTIR) of adsorbents characterized in our previous study [35]. Fig. 1 shows the scanning electron micrographs of adsorbent. The SEM micrograph of graphene displays very smooth and continuous surface with wrinkle edges. On the other hand, SEM micrograph of SMG shows very rough surface with discrete patterns. This attributes to the breakage of graphene structure after modification and presence of oxygen containing functional groups on its surface as shown in XRD and FTIR results (Table 1), respectively. Similarly, Ihsanullah et al. [33] found that acid treatment of activated carbon and CNT resulted in a rough surface. TGA was performed under nitrogen atmosphere to assess the thermal stability of G and SMG and are illustrated in Fig. 2. In case of SMG, the weight loss of 3% below 100°C ascribed the release of water vapor and about 9% at 200°C indicating the loss of CO, CO₂ due to the pyrolysis of oxygen functionalities. In contrast, the graphene shows very high thermal stability with no major reduction in mass up to 800°C. Table 2 shows the BET surface area, pore volume, and pore size of G and SMG. Nitrogen adsorption–desorption showed that acid modification of graphene increased surface area from 404 to 512.5 m²/g. However, there was no significant improvement in pore volume and pore size for the SMG compared with that of the G.

Fig. 3 shows the FTIR spectrum of SMG before and after Pb(II) adsorption. It was found that after adsorption of Pb(II) on the surface of SMG, the peaks at 1,620 and 1,260 cm⁻¹ corresponds to C=C and C–O–C groups, respectively, almost disappeared. Moreover, the intensity of peaks at 1,102 and

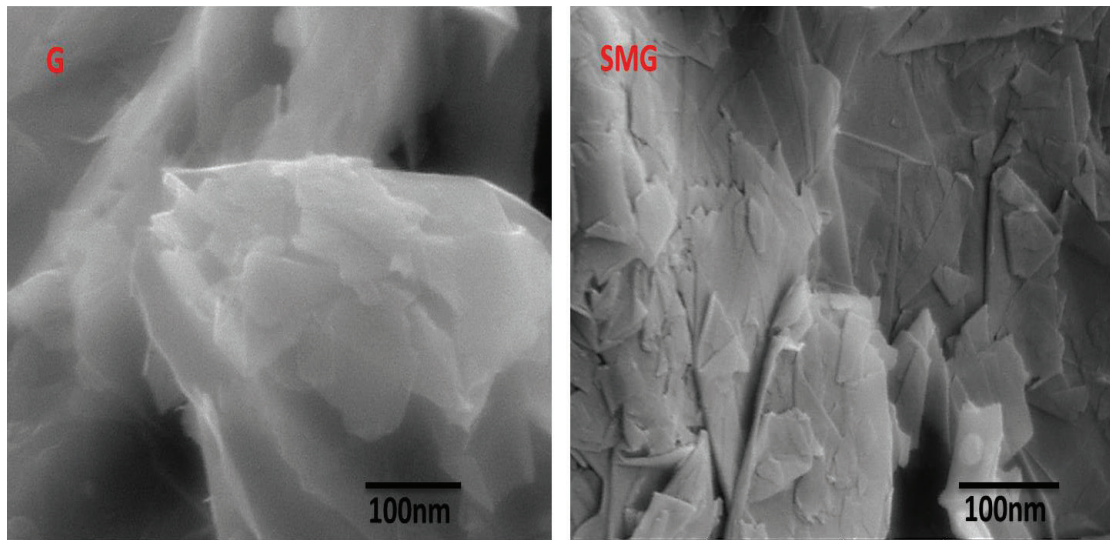


Fig. 1. SEM micrographs of graphene (G) and surface-modified graphene (SMG).

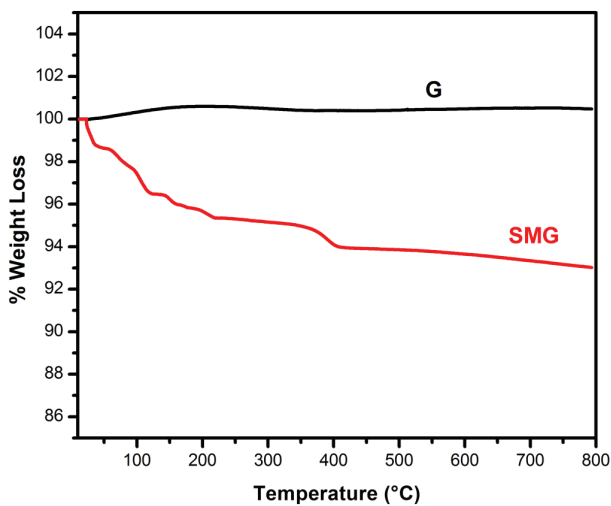


Fig. 2. TGA plots of G and SMG.

Table 2
Surface area, pore volume, and pore size of G and SMG

	G	SMG
BET surface area (m ² /g)	404	512.5
Pore volume (at $p/p_0 = 0.9725$) (cm ³ /g)	0.586	0.575
Pore size (based on Barrett-Joyner-Halenda) (Å)	46.47	46.46

1,016 cm⁻¹ associated to C–O group was lowered. This suggests that Pb(II) reacted with oxygen functionalities of SMG. Similar behaviour was also reported in previous studies [39,40]. The characterization results clearly support that surface modification of graphene using concentrated nitric acid was highly effective and expected to improve the active binding sites on the surface of SMG. This change in surface characteristic enhanced adsorption capacity of Pb(II) on SMG as demonstrated in Fig. 4.

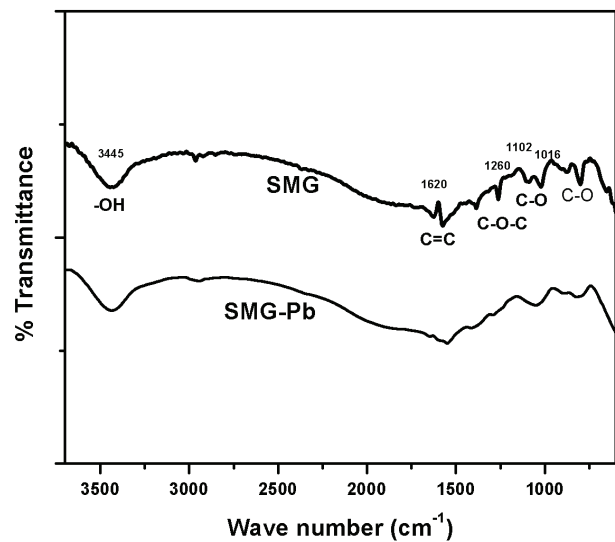


Fig. 3. FTIR spectra of SMG before and after Pb(II) adsorption.

3.2. Effect of studied parameters on Pb(II) adsorption

3.2.1. Effect of pH

Fig. 5(A) shows the effect of pH on adsorption capacity (q_e) of Pb(II) on G and SMG. Fig. 5(B) shows the points of zero charge (pH_{pzc}) of G and SMG determined by the pH drift method [41] which were found to be 5.5 and 4.7, respectively. Obviously, Fig. 5(A) shows that removal of Pb(II) by G and SMG was very low below pH of 4. Removal increased when pH was increased. The adsorption capacity of Pb(II) on G and SMG at pH 4 was 2.56 and 9.79 mg/g which was substantially increased to about 27.04 and 50.84 mg/g, respectively, at pH 7. The effect of pH on the adsorption of Pb(II) can be well explained on the basis of ionic chemistry of both adsorbate and adsorbents. Different studies demonstrated that sorption of neutral compounds is mostly associated to

the π - π interaction whereas cationic and anionic compounds adsorption is governed by electrostatic interactions [42,43]. At a pH of about 6, the predominant soluble species are Pb^{2+} , $Pb(OH)_2$, and $PbOH^+$, but between pH 7 and 12, the most common species are solid hydroxide and soluble $Pb(OH)^3-$, and $Pb(OH)_4^{2-}$ [44].

Very low adsorption capacity at $pH < 4$ was due to the presence of hydrogen ions on the surface of G and SMG as confirmed from point zero charge (Fig. 5(B)). These H^+ ions tend to cover the active sites of graphene surface and repel the Pb^{2+} due to electrostatic interactions. Consequently, the available number of active sites and efficiency of adsorption decreases. As the pH of the solution increases from 4 to 7, the surface of graphene exhibited lower H^+ ions and became negatively charged, above its pH_{pzc} . Thus, adsorption capacity significantly improved. Moreover, Fig. 5(A) demonstrates that the adsorption capacity of SMG was higher than that of G. For example, at a pH of 7, the adsorption capacity of Pb(II) was 27.04 and 50.84 mg/g by G and SMG, respectively. The improved adsorption tendency of SMG is attributed to the existence of oxygen functionalities and increased in the binding active sites on graphene surface after oxidation as confirmed from FTIR analysis (Fig. 3).

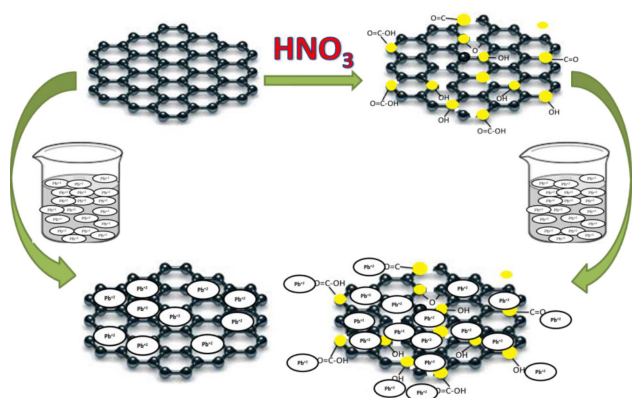


Fig. 4. Mechanism of improved adsorption capacity of Pb(II) on SMG.

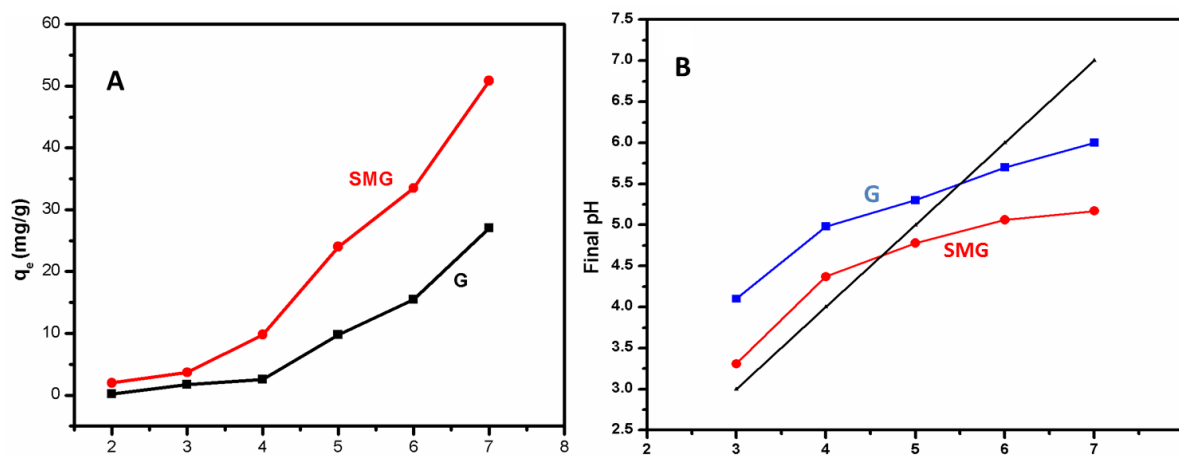


Fig. 5. (A) Effect of pH on adsorption of Pb(II) ion on G and SMG. Conditions: Co: 20 mg/L of Pb(II); adsorbent dosage 10 mg; time 180 min; temperature 298 K at pH 2–7. (B) Point zero charge of G and SMG.

These functional groups made SMG more hydrophilic and attracted the Pb(II) more efficiently and resulted in better uptake of Pb(II). Similar behaviour was also concluded in previous studies using modified CNT and activated carbon [32,45].

3.2.2. Effect of adsorbent dose

The batch experiment was carried out using varied proportions of G and SMG ranging from 4 to 32 mg while other parameters such as pH, contact time, and rpm were fixed. Fig. 6 shows that amount of adsorbent profoundly influenced the uptake of Pb(II) ions. The removal efficiency increased from 15% to 54% for G and from 32% to 83% for SMG when the adsorbent dose was increased from 4 to 20 mg. In all scenarios, SMG showed higher percentage removal of Pb(II) compared with G. This is attributed to greater surface area and abundance of interfacial sites available for adsorption after oxidation of graphene. At higher dose of adsorbents, more availability of interfacial sites for adsorption (i.e., exchangeable sites for ions interaction) was expected. However, the percentage removal of Pb(II) on both adsorbents did not increase after addition of 20 mg of adsorbent.

3.2.3. Effect of contact time

Fig. 7 displays the dependence of the Pb(II) adsorption capacity on contact time ranging from 5 to 180 min. Both adsorbents showed good adsorption of Pb(II) during the first 20 min, that is, adsorption capacity increased as the contact time increased (Fig. 7). Evidently, the adsorption of Pb(II) onto both G and SMG was very fast and equilibrium was achieved very quickly. Clearly, the trends showed that the adsorption of the Pb(II) ions was high within the first 60 min of the experiment. Afterwards, the adsorption rate decreased, apparently, due to the diminishing functional groups on the surface. Therefore, adsorption equilibrium was achieved in 100 and 80 min for G and SMG, respectively.

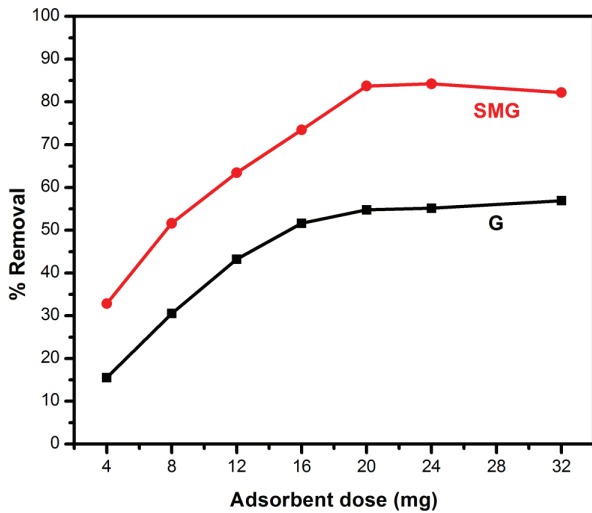


Fig. 6. Effect of adsorbent dosage on adsorption of Pb(II) ion on G and SMG. Conditions: Co: 20 mg/L of Pb(II); time 180 min; temperature 298 K at pH 6.5; adsorbent dosage 4–32 mg.

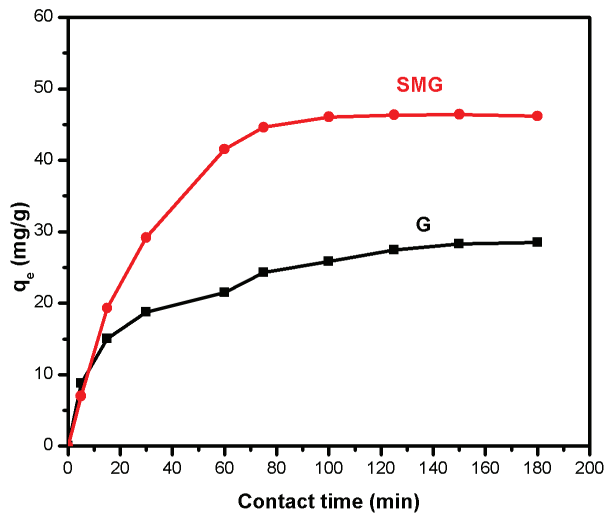


Fig. 7. Effect of contact time on adsorption of Pb(II) ion on G and SMG. Conditions: Co: 20 mg/L of Pb(II); temperature 298 K; pH 6.5; adsorbent dosage 10 mg at time 5–180 min.

3.2.4. Adsorption kinetics of lead

Adsorption is a multi-step process that involves external diffusion, internal diffusion, and surface reaction [25]. Usually in a well-mixed system of small adsorbents' particles as in the case of this study, external diffusion is not controlling the adsorption process. Intra-particle diffusion is assumed to play a key role in adsorption when the constant (C) is zero [46]. Fig. 8(C) and Table 3 confirm that intra-particle diffusion was not controlling the adsorption of Pb(II) on G and SMG. Noticeably, pseudo-second-order model (Fig. 8(B)) fitted much better the data than pseudo-first-order model (Fig. 8(A)), especially for SMG. The correlation coefficients using pseudo-second-order model were close to 1 and higher than those of pseudo-first-order model (Table 3).

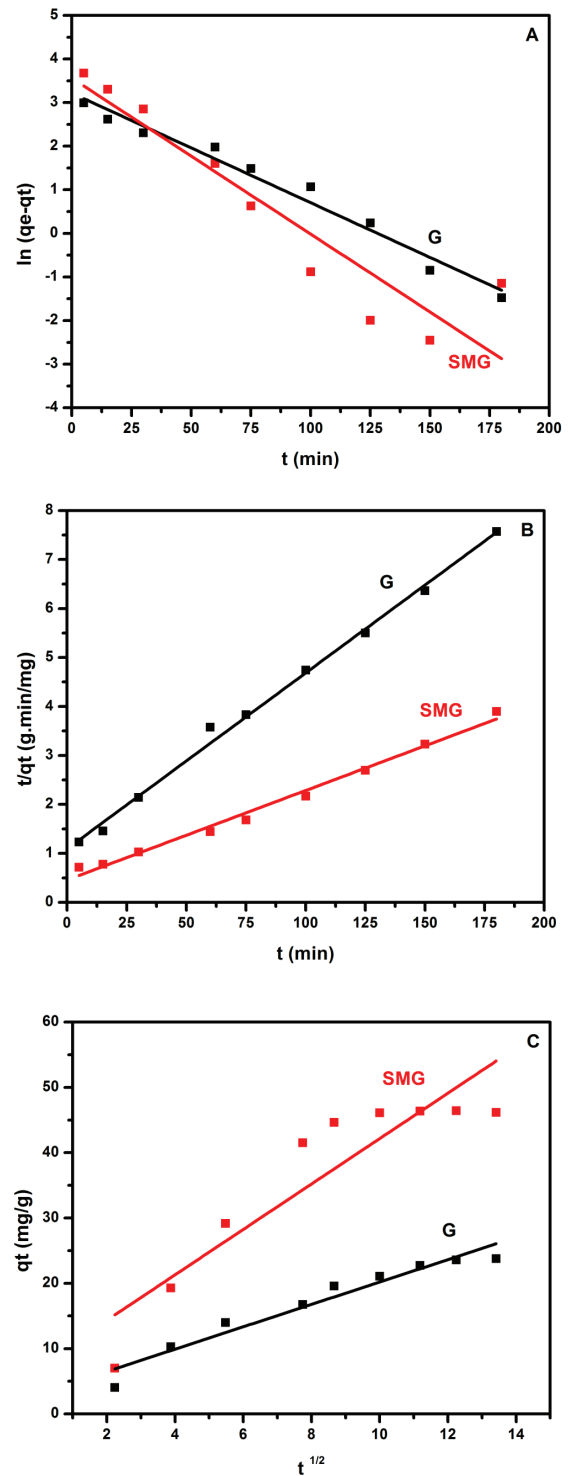


Fig. 8. Pseudo-first-order model (A), pseudo-second-order model (B), and intra-particle diffusion model (C).

Moreover, the calculated q_e agreed well with the experimental q_e value using pseudo-second-order model. This means that chemisorption was the main mechanism of adsorption of Pb(II) on G and SMG. Apparently, the presence of oxygen functionalities particularly on SMG surface played

Table 3

Kinetics parameters of pseudo-first-order, pseudo-second-order, and intra-particle diffusion model for Pb(II) adsorption on G and SMG

Kinetic models	Parameters	Adsorbent	
		G	SMG
Pseudo-first-order	k_1 (1/min)	0.025	0.035
$\ln(q_e - q_t) = \ln q_e - k_1 t$	q_e (mg/g)	24.779	35.128
	R^2	0.976	0.875
	Pseudo-second-order	k_2 (g/mg min)	1.20×10^{-3}
$\frac{t}{q_t} = \frac{t}{k_2 q_e^2} + \frac{t}{q_e}$	q_e (mg/g)	27.855	54.644
	R^2	0.995	0.990
	Intra-particle diffusion	k_i (mg/g min ^{1/2})	3.47
$q_t = k_p t^{1/2} + C$	C	7.393	3.23
	R^2	0.973	0.840

a key role and likely to be the rate controlling step in our graphene–Pb interaction process.

3.2.5. Adsorption isotherm of lead

Fig. 9(A) shows that Langmuir isotherm fitted very well the experimental data ($R^2 > 0.98$, Table 4). The values of q_m and b were estimated from the slope and intercept of Fig. 9(A). The monolayer adsorption capacity (q_m) was 69.98 and 140.44 mg/g for G and SMG, respectively. The increase in monolayer adsorption capacity (q_m) of SMG compared with G is attributed to two reasons (i) existence of functional groups on the graphene surface and (ii) higher surface area of SMG compared with G. The nature of Langmuir isotherm plot reveals whether the adsorption process is favourable or not. The values of equilibrium constant R_L for G and SMG were 0.12 and 0.18, respectively, which confirmed that the adsorption of Pb(II) on both adsorbents was favourable, but reversible.

Similarly, Freundlich isotherm fitted very well the results (Fig. 9(B)) with a correlation coefficient R^2 near to 1 for both adsorbents (Table 4). It is well known that Freundlich isotherm describes well the adsorption on heterogeneous surface [47]. Obviously, SEM micrographs showed that G and SMG were heterogeneous in nature (Fig. 1). Freundlich constants, k_f and n , are the indicative of adsorption tendency of adsorbent and percentage of heterogeneity with degree of adsorption affinity, respectively [48]. The values of $1/n$, listed in Table 3 for G and SMG to be 0.346 and 0.449, respectively, indicated that the adsorption of Pb(II) was favourable (i.e., $1 < n < 10$) [47].

Expectedly, Redlich–Peterson model fitted the data with a correlation coefficient of almost 1 (Fig. 9(C) and Table 4) because the model is built based on both Langmuir and Freundlich models, where both fitted the results [49]. Moreover, Redlich–Peterson model contains three empirical parameters. The values of b_R for G and SMG were 0.684 and 0.573, respectively, which means that graphene had both homogenous and heterogeneous adsorption sites.

Table 5 compares the adsorption capacity of G and SMG with other related carbon materials. The adsorption capacity

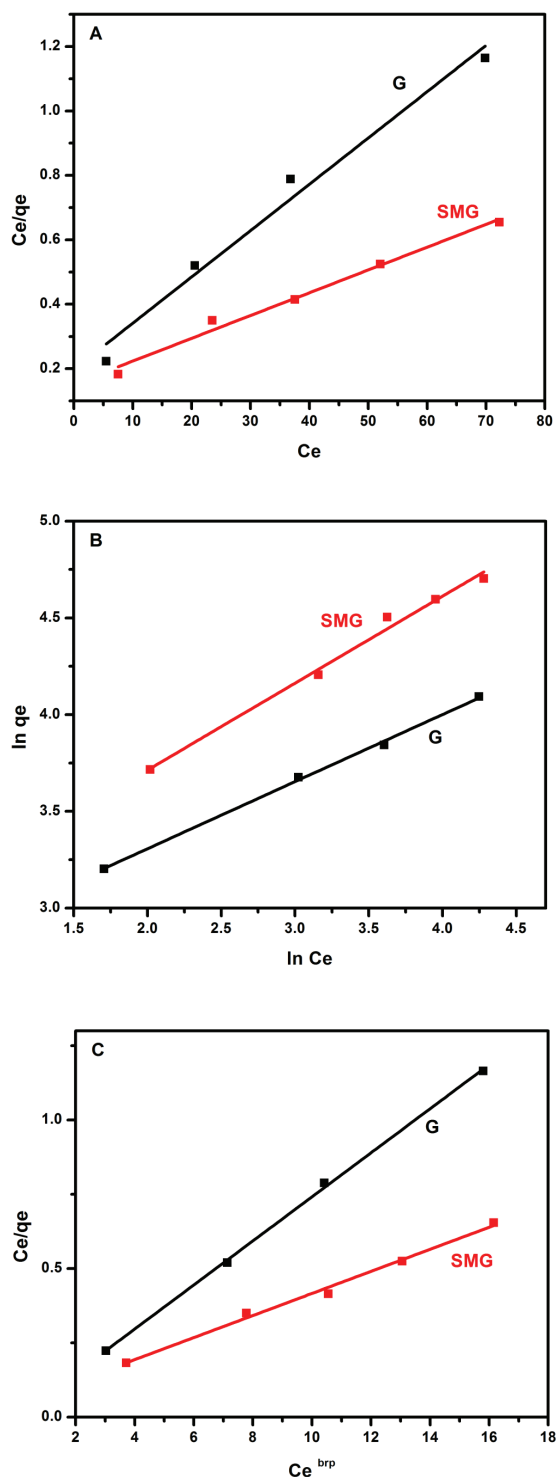


Fig. 9. Langmuir isotherm model (A), Freundlich isotherm model (B), and Redlich–Peterson model (C).

of G was within the range of maximum adsorption capacities in literature. However, SMG was a superior adsorbent compared with other adsorbents (Table 5). Therefore, SMG can be used in adsorption process to efficiently remove heavy metal ions from water.

Table 4
Estimated isotherm parameters for Langmuir, Freundlich, and Redlich–Peterson models for adsorption of Pb(II) on G and SMG

Isotherms	Adsorbent	Constants		
Langmuir		q_m (mg/g)	b (l/mg)	R^2
	G	69.44	0.072	0.981
	SMG	140.84	0.046	0.987
Freundlich		K_f (mg/g)	$1/n$	
	G	13.64	0.346	0.998
	SMG	28.50	0.449	0.991
Redlich–Peterson		b_R	a_R	
	G	0.684	3.18	0.999
	SMG	0.573	4.39	0.994

Table 5
Comparison of maximum adsorption capacity (q_{max}) of Pb(II) on other carbon materials at 298 K

Adsorbent	q_{max} (mg/g)	pH	t (min)	References
Activated carbon from coconut shell	92.39	5	120	[50]
Raw multi wall carbon nanotubes (MWCNT)	2.94	6	120	[32]
Oxidized MWCNT	37.36	6	120	[32]
CNT	102.04	5	120	[51]
Magnetic multi-walled carbon nanotubes	67.25	5	120	[52]
Graphite oxide	60.5	6.2	120	[53]
Graphene oxide	111.1	6	60	[54]
Graphene nanosheets	35.7	6	120	[55]
Tartaric acid-modified graphene	107.74	6	30	[34]
Raw graphene (G)	69.77	6.5	100	Our study
Surface-modified graphene (SMG)	140.84	6.5	80	Our study

4. Conclusion

In this study, graphene (G) was chemically modified using nitric acid to improve its adsorption capacity. The adsorption capacities of G and SMG, for the removal of Pb(II) from aqueous solution, were measured at different operating conditions. Maximum removal of Pb(II) on both adsorbents were found between pH 6 and 7, contact time of 80–120 min, and adsorbent dose of 20 mg at 250 rpm and 298 K. BET surface area of SMG was 512.5 m²/g compared with 404 m²/g of G. The adsorption capacity of SMG was 140 mg/g which was two folds the capacity obtained by G, implying that the chemical modification of G was very efficient for Pb(II) sorption. Pseudo-second-order fitted very well the adsorption results, indicating that the mechanism of adsorption was chemisorption. Equilibrium data were explained using Langmuir, Freundlich, and Redlich–Peterson isotherm models. All the models fitted very well the results with correlation coefficient (R^2) close to 1. These results demonstrated the potentials of SMG as a superior adsorbent for the removal of heavy metal ions from aqueous solutions.

References

- [1] B.A. Chowdhury, R.K. Chandra, Biological and health implications of toxic heavy metal and essential trace element interactions, *Prog. Food Nutr. Sci.*, 11 (1987) 55–113.
- [2] S. Davydova, Heavy metals as toxicants in big cities, *Microchem. J.*, 79 (2005) 133–136.
- [3] R.A. Wuana, F.E. Okieimen, Heavy metals in contaminated soils: a review of sources, chemistry, risks and best available strategies for remediation, *ISRN Ecol.*, 2011 (2011) 20.
- [4] S.M. Mousa, N.S. Ammar, H.A. Ibrahim, Removal of lead ions using hydroxyapatite nano-material prepared from phosphogypsum waste, *J. Saudi Chem. Soc.*, 20 (2016) 357–365.
- [5] WHO, Guidelines for Drinking Water Quality, Switzerland, 1984, pp. 1–2.
- [6] M.M. Matlock, B.S. Howerton, D.A. Atwood, Chemical precipitation of lead from lead battery recycling plant wastewater, *Ind. Eng. Chem. Res.*, 41 (2002) 1579–1582.
- [7] A.R. Karbassi, S. Nadjafpour, Flocculation of dissolved Pb, Cu, Zn and Mn during estuarine mixing of river water with the Caspian Sea, *Environ. Pollut.*, 93 (1996) 257–260.
- [8] M. Naushad, A. Mittal, M. Rathore, V. Gupta, Ion-exchange kinetic studies for Cd(II), Co(II), Cu(II), and Pb(II) metal ions over a composite cation exchanger, *Desal. Wat. Treat.*, 54 (2015) 2883–2890.
- [9] M. Soyulak, Y.E. Unsal, N. Kizil, A. Aydin, Utilization of membrane filtration for preconcentration and determination of Cu(II) and Pb(II) in food, water and geological samples by atomic absorption spectrometry, *Food Chem. Toxicol.*, 48 (2010) 517–521.
- [10] M. Zubair, N. Jarrah, M.S. Manzar, M. Al-Harathi, M. Daud, N.D. Mu'azu, S.A. Haladu, Adsorption of eriochrome black T from aqueous phase on MgAl-, CoAl- and NiFe- calcined layered double hydroxides: kinetic, equilibrium and thermodynamic studies, *J. Mol. Liq.*, 230 (2017) 344–352.

- [11] J. Goel, K. Kadirvelu, C. Rajagopal, V. Kumar Garg, Removal of lead(II) by adsorption using treated granular activated carbon: batch and column studies, *J. Hazard. Mater.*, 125 (2005) 211–220.
- [12] J. Perić, M. Trgo, N. Vukojević Medvidović, Removal of zinc, copper and lead by natural zeolite—a comparison of adsorption isotherms, *Water Res.*, 38 (2004) 1893–1899.
- [13] R. Naseem, S.S. Tahir, Removal of Pb(II) from aqueous/acidic solutions by using bentonite as an adsorbent, *Water Res.*, 35 (2001) 3982–3986.
- [14] T.K. Das, S. Prusty, Recent advances in application of graphene, *Int. J. Chem. Sci. Appl.*, 4 (2013) 39–55.
- [15] M. Zubair, J. Jose, M.A. Al-Harhi, Evaluation of mechanical and thermal properties of microwave irradiated poly (styrene-co-methyl methacrylate)/graphene nanocomposites, *Compos. Interfaces*, 22 (2015) 595–610.
- [16] M. Zubair, F. Shehzad, M.A. Al-Harhi, Impact of modified graphene and microwave irradiation on thermal stability and degradation mechanism of poly (styrene-co-methyl methacrylate), *Thermochim. Acta*, 633 (2016) 48–55.
- [17] M.A. Al-Harhi, M. Zubair, Effect of Modified Graphene and Microwave Irradiation on the Mechanical and Thermal Properties of P(S-co-MMA)/Graphene Nanocomposites, Google Patents, 2016.
- [18] K. Rana, J. Singh, J.-H. Ahn, A graphene-based transparent electrode for use in flexible optoelectronic devices, *J. Mater. Chem.*, 2 (2014) 2646–2656.
- [19] Z. Yin, S. Sun, T. Salim, S. Wu, X. Huang, Q. He, Y.M. Lam, H. Zhang, Organic photovoltaic devices using highly flexible reduced graphene oxide films as transparent electrodes, *ACS Nano*, 4 (2010) 5263–5268.
- [20] L. Fan, C. Luo, M. Sun, X. Li, H. Qiu, Highly selective adsorption of lead ions by water-dispersible magnetic chitosan/graphene oxide composites, *Colloids Surf., B*, 103 (2013) 523–529.
- [21] J. Hur, J. Shin, J. Yoo, Y.-S. Seo, Competitive adsorption of metals onto magnetic graphene oxide: comparison with other carbonaceous adsorbents, *Sci. World J.*, 2015 (2015) 11.
- [22] G. Kyzas, N. Travlou, O. Kalogirou, E. Deliyanni, Magnetic graphene oxide: effect of preparation route on Reactive Black 5 adsorption, *Materials*, 6 (2013) 1360–1376.
- [23] G.Z. Kyzas, E.A. Deliyanni, K.A. Matis, Graphene oxide and its application as an adsorbent for wastewater treatment, *J. Chem. Technol. Biotechnol.*, 89 (2014) 196–205.
- [24] G.K. Ramesha, A. Vijaya Kumara, H.B. Muralidhara, S. Sampath, Graphene and graphene oxide as effective adsorbents toward anionic and cationic dyes, *J. Colloid Interface Sci.*, 361 (2011) 270–277.
- [25] X. Deng, L. Lü, H. Li, F. Luo, The adsorption properties of Pb(II) and Cd(II) on functionalized graphene prepared by electrolysis method, *J. Hazard. Mater.*, 183 (2010) 923–930.
- [26] D. Dinda, A. Gupta, S.K. Saha, Removal of toxic Cr(vi) by UV-active functionalized graphene oxide for water purification, *J. Mater. Chem. A*, 1 (2013) 11221–11228.
- [27] V.K. Gupta, O. Moradi, I. Tyagi, S. Agarwal, H. Sadegh, R. Shahryari-Ghoshekandi, A.S.H. Makhlof, M. Goodarzi, A. Garshasbi, Study on the removal of heavy metal ions from industry waste by carbon nanotubes: effect of the surface modification: a review, *Crit. Rev. Environ. Sci. Technol.*, 46 (2016) 1–26.
- [28] A.K. Mishra, S. Ramaprabhu, Functionalized graphene sheets for arsenic removal and desalination of sea water, *Desalination*, 282 (2011) 39–45.
- [29] J. Azamat, B.S. Sattary, A. Khataee, S.W. Joo, Removal of a hazardous heavy metal from aqueous solution using functionalized graphene and boron nitride nanosheets: insights from simulations, *J. Mol. Graphics Modell.*, 61 (2015) 13–20.
- [30] A. Murugesan, T. Vidhyadevi, S.S. Kalaivani, P. Baskaralingam, C.D. Anuradha, S. Sivanesan, Kinetic studies and isotherm modeling for the removal of Ni²⁺ and Pb²⁺ ions by modified activated carbon using sulfuric acid, *Environ. Prog. Sustainable Energy*, 33 (2014) 844–854.
- [31] A. Deliyanni Eleni, Z. Kyzas George, S. Triantafyllidis Kostas, A. Matis Kostas, Activated carbons for the removal of heavy metal ions: a systematic review of recent literature focused on lead and arsenic ions, *Open Chem.*, 13 (2015). doi: <https://doi.org/10.1515/chem-2015-0087>
- [32] G.D. Vuković, A.D. Marinković, S.D. Škapin, M.D. Ristić, R. Aleksić, A.A. Perić-Grujić, P.S. Uskoković, Removal of lead from water by amino modified multi-walled carbon nanotubes, *Chem. Eng. J.*, 173 (2011) 855–865.
- [33] Ihsanullah, F.A. Al-Khaldi, B. Abu-Sharkh, A.M. Abulkibash, M.I. Qureshi, T. Laoui, M.A. Atieh, Effect of acid modification on adsorption of hexavalent chromium (Cr(VI)) from aqueous solution by activated carbon and carbon nanotubes, *Desal. Wat. Treat.*, 57 (2016) 7232–7244.
- [34] Z.-H. Wang, B.-Y. Yue, J. Teng, F.-P. Jiao, X.-Y. Jiang, J.-G. Yu, M. Zhong, X.-Q. Chen, Tartaric acid modified graphene oxide as a novel adsorbent for high-efficiently removal of Cu(II) and Pb(II) from aqueous solutions, *J. Taiwan Inst. Chem. Eng.*, 66 (2016) 181–190.
- [35] M. Zubair, J. Jose, A.-H. Emwas, M.A. Al-Harhi, Effect of modified graphene and microwave irradiation on the mechanical and thermal properties of poly(styrene-co-methyl methacrylate)/graphene nanocomposites, *Surf. Interface Anal.*, 46 (2014) 630–639.
- [36] Y.S. Ho, G. McKay, A comparison of chemisorption kinetic models applied to pollutant removal on various sorbents, *Process Saf. Environ. Prot.*, 76 (1998) 332–340.
- [37] Z. Zhu, W. Li, Efficient adsorption and desorption of Pb²⁺ from aqueous solution, *J. Environ. Chem. Eng.*, 1 (2013) 838–843.
- [38] F. Ogata, N. Kawasaki, Adsorption of Pt(IV) and Pd(II) by calcined dried aluminum hydroxide gel from aqueous solution system, *J. Environ. Chem. Eng.*, 1 (2013) 1013–1019.
- [39] X. Yang, X. Cui, Adsorption characteristics of Pb (II) on alkali treated tea residue, *Water Resour. Ind.*, 3 (2013) 1–10.
- [40] D.J. Amorim, H.C. Rezende, É.L. Oliveira, I.L.S. Almeida, N.M.M. Coelho, T.N. Matos, C.S.T. Araújo, Characterization of Pequi (*Caryocar brasiliense*) shells and evaluation of their potential for the adsorption of Pb(II) ions in aqueous systems, *J. Braz. Chem. Soc.*, 27 (2016) 616–623.
- [41] M.A. Atieh, O.Y. Bakather, B.S. Tawabini, A.A. Bukhari, M. Khaled, M. Alharhi, M. Fettouhi, F.A. Abuilwaiwi, Removal of chromium (III) from water by using modified and nonmodified carbon nanotubes, *J. Nanomater.*, 2010 (2010) 1–9.
- [42] K. Pyrzynska, Carbon nanostructures for separation, preconcentration and speciation of metal ions, *Trends Anal. Chem.*, 29 (2010) 718–727.
- [43] C. Moreno-Castilla, Adsorption of organic molecules from aqueous solutions on carbon materials, *Carbon*, 42 (2004) 83–94.
- [44] L. Giraldo, J. Moreno-Piraján, Pb²⁺ adsorption from aqueous solutions on activated carbons obtained from lignocellulosic residues, *Braz. J. Chem. Eng.*, 25 (2008) 143–151.
- [45] S. Yao, J. Zhang, D. Shen, R. Xiao, S. Gu, M. Zhao, J. Liang, Removal of Pb(II) from water by the activated carbon modified by nitric acid under microwave heating, *J. Colloid Interface Sci.*, 463 (2016) 118–127.
- [46] Y.-H. Li, S. Wang, Z. Luan, J. Ding, C. Xu, D. Wu, Adsorption of cadmium(II) from aqueous solution by surface oxidized carbon nanotubes, *Carbon*, 41 (2003) 1057–1062.
- [47] M. Avila, T. Burks, F. Akhtar, M. Göthelid, P.C. Lansåker, M.S. Toprak, M. Muhammed, A. Uheida, Surface functionalized nanofibers for the removal of chromium(VI) from aqueous solutions, *Chem. Eng. J.*, 245 (2014) 201–209.
- [48] M.H. Dehghani, M.M. Taher, A.K. Bajpai, B. Heibati, I. Tyagi, M. Asif, S. Agarwal, V.K. Gupta, Removal of noxious Cr (VI) ions using single-walled carbon nanotubes and multi-walled carbon nanotubes, *Chem. Eng. J.*, 279 (2015) 344–352.
- [49] K.Y. Foo, B.H. Hameed, Insights into the modeling of adsorption isotherm systems, *Chem. Eng. J.*, 156 (2010) 2–10.
- [50] M. Caccin, M. Giorgi, F. Giacobbo, M. Da Ros, L. Besozzi, M. Mariani, Removal of lead (II) from aqueous solutions by adsorption onto activated carbons prepared from coconut shell, *Desal. Wat. Treat.*, 57 (2016) 4557–4575.
- [51] N.A. Kabbashi, M.A. Atieh, A. Al-Mamun, M.E.S. Mirghami, M.D.Z. Alam, N. Yahya, Kinetic adsorption of application of carbon nanotubes for Pb(II) removal from aqueous solution, *J. Environ. Sci.*, 21 (2009) 539–544.

- [52] L. Jiang, H. Yu, X. Zhou, X. Hou, Z. Zou, S. Li, C. Li, X. Yao, Preparation, characterization, and adsorption properties of magnetic multi-walled carbon nanotubes for simultaneous removal of lead(II) and zinc(II) from aqueous solutions, *Desal. Wat. Treat.*, 57 (2016) 18446–18462.
- [53] O. Olanipekun, A. Oyefusi, G.M. Neelgund, A. Oki, Adsorption of lead over graphite oxide, *Spectrochim. Acta Part A*, 118 (2014) 857–860.
- [54] M. Yari, M. Norouzi, A.H. Mahvi, M. Rajabi, A. Yari, O. Moradi, I. Tyagi, V.K. Gupta, Removal of Pb(II) ion from aqueous solution by graphene oxide and functionalized graphene oxide-thiol: effect of cysteamine concentration on the bonding constant, *Desal. Wat. Treat.*, 57 (2016) 11195–11210.
- [55] Z.-H. Huang, X. Zheng, W. Lv, M. Wang, Q.-H. Yang, F. Kang, Adsorption of lead(II) ions from aqueous solution on low-temperature exfoliated graphene nanosheets, *Langmuir*, 27 (2011) 7558–7562.